WOOD RESEARCH
62 (3): 2017
341-352

KALMAN FILTERING OF GAUGES NOISE ON THE CREEP BEHAVIOR OF *ENTANDROPHRAGMA CYLINDRICUM* (SAPELLI) UNDER A CONSTANT STRESS

Pierre Kisitotalla, Prisca Kuida Atchounga, Blaise Mtopi
University of Dschang, Department of Physics
Laboratory of Mechanics and Modelling of Physical Systems (*L2MSP*)
Dschang, Cameroon

(Received August 2016)

ABSTRACT

In this work, we drew the experimental or the true creep-recovery curves of *Entandrophragma cylindricum* known as sapelli from the values obtained during many four points flexural tests carried out on several samples of this hardwood. Thereafter, the experimental values have been perturbed by the white Gaussian noise of the gauges and this allowed us to draw the noisy curves of deformations. The creep test lasted ten hours and the recovery forty hours. Our main target in this work was to implement the recursive discrete Kalman filter, in order to predict or to estimate the deformation of this species undergoing a constant stress. From the simulation, since our estimate and our state have the same expected value, then our estimate is not biased. The true deformation and the estimated deformation curves are almost too close to distinguish from one another. Once the Kalman filter applied to our system satisfied these two preceding criteria, we are able to mention that our estimator has a good response therefore, it is an optimal filter.

KEYWORDS: Creep, discrete Kalman filter, Gaussian white noise, linear stochastic difference equation, recovery, stress.

INTRODUCTION

Entandrophragma cylindricum referred to as sapelli is a forestry species encountered mostly in west and central African forests. In Cameroon this wood is widely exploited in several domains. For example, in many localities bridges, houses and pigsty are built with this material and their lifespan is significant. Physical and mechanical properties of this species have already been the subject of extensive research (Mvogo 2008). But from the bibliography we explored, neither the creep behavior of this biomaterial under a constant stress nor the prediction of its lifespan via a powerful means as the Kalman filter have not yet received particular attention. Considering the importance of this biomaterial in our society, it is of paramount interest to study the effect

of gauges noise on its creep behavior through flexural tests on some samples. Whatever the gauge considered, its working is seriously influenced by parasitical effects like the temperature, the hysteresis phenomenon and the linearity errors of the maker. When a gauge is fixed on a sample of wood, it undergoes deformations following the proper dilatation of the material due to thermal effects; this is because both the gauge and the sample do not have the same thermal dilatation coefficient. Besides, during the creep it is impossible to foresee the thermal effect on the connection cables of the gauges which generates serious fluctuations on the deformation (Bertholet and Fanchon 1974). We can also underline the fluctuations generated by the supply voltage that perturbs the creep. The true deformation which is the useful information became drown in the generated noise.

This work is a part of an effort to build a dynamic data application system for hardwoods. The method proposed in this paper was motivated by the observation that straightforward application of Burger and Schapery models to prediction of creep behavior of biomaterials (Talla et al. 2010) always failed, because the models did not take into consideration the fluctuations of temperature, humidity and mainly the noise of sensors which perturb seriously the deformations. The discrete Kalman filter appears as the ideal model and tool to solve this problem, because it can remove the undesired noise from our useful deformation and it also takes into consideration estimation of past, present and even future states (Fortunier 1998). Besides, due to the fact that the creep is a lasting phenomenon, it becomes more difficult and boring for an experimenter to measure manually the deformation of the material over a large scale of time. The Kalman filter also being a powerful predicting tool then, knowing some experimental values at the beginning of the creep test, the filter can predict the creep behavior of the material over a large scale of time while minimizing the estimation error. This method is time gaining for the experimenter and it also allows him to avoid accident risks that may occur during the test with devices. Four points' flexural tests have been first carried out on three samples of our species; thereafter the experimental values of deformation collected allowed us to build true, noisy and estimated Kalman curves of creep recovery of the hardwood.

Theories of flexural deformation and Kalman filter

Theory of flexural deformation

In four-points bending, the maximum tensile stress occurs at the middle of the bottom area of the beam and compressive stress at the top. Likewise, in this zone, the deflection is maximum (Pramanick and Sain 2006). In the below figure, P is the applied load, L the span of beam and L/3 distance between the points of application of load and the support.

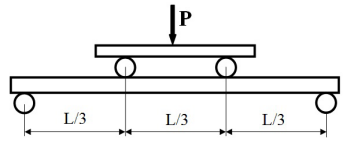

Fig.1: A typical four-point bending.

The corresponding maximum deflection at the middle of the beam is obtaining by:

$$f_{\max} = \frac{23}{1296}\frac{PL^3}{EI} \tag{1}$$

Where the quantity E represents the young modulus of the beam and I stands for its quadratical moment of inertia.

Theory of discrete Kalman filter

In 1960 Kalman published his paper describing a recursive solution to the discrete-data linear filtering problem (Greg and Bishop 2006). Since that time, due in large part to advances in digital computing; the Kalman filter has been the subject of extensive research and application, particularly in the area of autonomous or assisted navigation.

The process to be estimated

The Kalman filter addresses the general problem of trying to estimate the state x of a discrete-time controlled process that is governed by the linear stochastic difference equation

$$x_{k+1} = Ax_k + Bu_k + w_k \tag{2}$$

With a measurement equation

$$y_k = Hx_k + v_k \tag{3}$$

The random variables wk and vk represent the process and measurement noises respectively. They are assumed to be independent of each other, white and with normal probability distributions (Evensen 2003). A white noise is a stochastic process with autocorrelation different from zero only at the origin but zero everywhere. It is a de-correlated process.

$$p(w) = N(0, Q) \text{ and } p(v) = N(0, R) \text{ with } Q = E\left[w_k w_k^T\right] \text{ and } R = E\left[v_k v_k^T\right] \tag{4}$$

Here, we assume constant the *process noise covariance* Q and *measurement noise covariance R* matrices.

In the above equations A, B and H are constant matrices, ***k*** is the time index; ***x*** is called the state of the system; ***u*** is a known input to the system and ***y*** is the measured output vector. The vector ***x*** contains all of the information about the present state of the system, but we cannot measure ***x*** directly. Instead we measure ***y***, which is a function of ***x*** that is corrupted by the noise *v*. We can use ***y*** to help us obtain an estimate of ***x***, but we cannot necessarily take the information from y at face value because it is corrupted by noise.

The computational origins of the filter

We define $\hat{x}_k^-$ to be our a priori state estimate at step k given knowledge of the process prior to step k, and $\hat{x}_k^+$ to be our a posteriori state estimate at step k given measurement y_k. We can define a priori and a posteriori estimate errors as

$$e_k^- \equiv x_k - \hat{x}_k^- \text{ and } e_k^+ \equiv x_k - \hat{x}_k^+ \tag{5}$$

The a priori estimate error covariance is then

$$P_k^- = E\left[e_k^- e_k^{-T}\right] \tag{6}$$

And the a posteriori estimate error covariance is

$$P_k^+ = E\left[e_k^+ e_k^{+T}\right] \tag{7}$$

In deriving the equations for the Kalman filter, we begin with the goal of finding an equation that computes an a posteriori state estimate $\hat{x}_k^+$ as a linear combination of an a priori estimate $\hat{x}_k^-$ and a weighted difference between an actual measurement y_k and a measurement prediction $H\hat{x}_k^-$ as shown below Eq. (8)

$$\hat{x}_k^+ = \hat{x}_k^- + K\left(y_k - H\hat{x}_k^-\right) \tag{8}$$

The difference $\left(y_k - H\hat{x}_k^-\right)$ is called the measurement innovation, or the residual. The matrix K in (8) is chosen to be the Kalman gain that minimizes the a posteriori error covariance (7). One popular form of the resulting K that minimizes (7) is given by (Hwang et al. 1992)

$$K_k = P_k^- H^T \left(HP_k^- H^T + R\right)^{-1} \tag{9}$$

The discrete Kalman filter algorithm

The Kalman filter estimates a process by using a form of feedback control: The filter estimates the process state at some time and then obtains feedback in the form of noisy measurements. As such, the equations for the Kalman filter fall into two groups: time update equations also called predictor equations and measurement update equations referred to as corrector equations. The predictor equations are responsible for projecting forward the current state and error covariance estimates to obtain the a priori estimates for next time step. The corrector equations are responsible for the feedback (Welch and Bishop 2006).

The specific equations for the prediction step are the following:

$$\hat{x}_{k+1}^- = A\hat{x}_k + Bu_k \tag{10}$$

$$P_{k+1}^- = AP_kA^T + Q \tag{11}$$

The specific corrector equations are the following:

$$K_{k+1} = P_{k+1}^- H^T \left(HP_{k+1}^- H^T + R\right)^{-1} \tag{12}$$

$$\hat{x}_{k+1}^+ = \hat{x}_{k+1}^- + K_{k+1}\left(y_k - H\hat{x}_{k+1}^-\right) \tag{13}$$

$$P_{k+1}^+ = P_{k+1}^- - K_{k+1}HP_{k+1}^- \tag{14}$$

Modeling of the dynamic system

Let $\varepsilon, \dot{\varepsilon}$ and $\ddot{\varepsilon}$ be respectively the deformation, the speed of deformation and the acceleration of the sample of wood undergoing a constant stress σ. We are collecting the deformation during the creep after each T seconds. From our knowledge in mathematics, we can express the deformation at the time k+1 as below:

$$\varepsilon_{k+1} = \varepsilon_k + T\dot{\varepsilon}_k + \frac{T^2}{2}\ddot{\varepsilon}_k + \tilde{\varepsilon}_k \tag{15}$$

here $\tilde{\varepsilon}_k$ is the white noise of gauges that perturbs the deformation. The speed of deformation at the same time can be derived from the preceding formula as:

$$\dot{\varepsilon}_{k+1} = \dot{\varepsilon}_k + T\ddot{\varepsilon}_k + \tilde{\dot{\varepsilon}}_k \tag{16}$$

In this relation the speed of deformation is perturbed by the white noise $\tilde{\dot{\varepsilon}}_k$.

Let $x_k = \begin{pmatrix} \varepsilon_k \\ \dot{\varepsilon}_k \end{pmatrix}$ and $x_{k+1} = \begin{pmatrix} \varepsilon_{k+1} \\ \dot{\varepsilon}_{k+1} \end{pmatrix}$ be the state vector respectively at the time k and k+1. ..

$w_k = \begin{pmatrix} \tilde{\varepsilon}_k \\ \tilde{\dot{\varepsilon}}_k \end{pmatrix}$ represents the state noise vector. Eqs. (16) and (17) can be written in the following form:

$$\begin{pmatrix} \varepsilon_{k+1} \\ \dot{\varepsilon}_{k+1} \end{pmatrix} = \begin{pmatrix} 1 & T \\ 0 & 1 \end{pmatrix}\begin{pmatrix} \varepsilon_k \\ \dot{\varepsilon}_k \end{pmatrix} + \begin{pmatrix} T^2/2 \\ T \end{pmatrix}\ddot{\varepsilon}_k + \begin{pmatrix} \tilde{\varepsilon}_k \\ \tilde{\dot{\varepsilon}}_k \end{pmatrix} \tag{17}$$

From this relation we can derive the state transition matrix A and the control matrix B as:

$$A = \begin{pmatrix} 1 & T \\ 0 & 1 \end{pmatrix} \text{ and } B = \begin{pmatrix} T^2/2 \\ T \end{pmatrix} \tag{18}$$

Let us look for the observation matrix H referred to as the measure matrix:

In the following system of equation, ε_1 is the measure of the deformation perturbed by the measurement noise b_1 and $\dot{\varepsilon}_1$ is the measure of the speed of deformation perturbed by the measurement noise b_2.

$$\varepsilon_1 = \varepsilon_k + b_1 \text{ and } \dot{\varepsilon}_1 = \dot{\varepsilon}_k + b_2 \tag{19}$$

Let $y_k = \begin{pmatrix} \varepsilon_1 \\ \dot{\varepsilon}_1 \end{pmatrix}$ be the measurement vector and $v_k = \begin{pmatrix} b_1 \\ b_2 \end{pmatrix}$ the measurement noise vector.

$$\begin{pmatrix} \varepsilon_1 \\ \dot{\varepsilon}_1 \end{pmatrix} = \begin{pmatrix} 1 & 0 \\ 0 & 1 \end{pmatrix} \begin{pmatrix} \varepsilon_k \\ \dot{\varepsilon}_k \end{pmatrix} + \begin{pmatrix} b_1 \\ b_2 \end{pmatrix} \tag{20}$$

It is straightforward from this relation that the observation matrix is

$$H = \begin{pmatrix} 1 & 0 \\ 0 & 1 \end{pmatrix} \tag{21}$$

We are now looking for the process noise covariance Q and measurement noise covariance R matrices that match well our system. They are defined by the following relations:

$$Q = E\left(w_k w_k^T\right) = E\left[\begin{pmatrix} \tilde{\varepsilon} \\ \tilde{\dot{\varepsilon}} \end{pmatrix}\begin{pmatrix} \tilde{\varepsilon} & \tilde{\dot{\varepsilon}} \end{pmatrix}\right] = E\begin{pmatrix} \tilde{\varepsilon}^2 & \tilde{\varepsilon}\tilde{\dot{\varepsilon}} \\ \tilde{\dot{\varepsilon}}\tilde{\varepsilon} & \tilde{\dot{\varepsilon}}^2 \end{pmatrix} \tag{22}$$

$$R = E\left(v_k v_k^T\right) = E\left[\begin{pmatrix} b_1 \\ b_2 \end{pmatrix}\begin{pmatrix} b_1 & b_2 \end{pmatrix}\right] = E\begin{pmatrix} b_1^2 & b_2 b_1 \\ b_1 b_2 & b_2^2 \end{pmatrix} \tag{23}$$

Where the capital letter E stands for the expectation value.

MATERIAL AND METHODS

The material used is the Sapelli, of scientific name *Entandrophragma cylindricum*. Our study was done on three samples well dried of this species from Cameroon forest. The selected samples did not have any macroscopically observable defect. They were all rectangular and had 34 cm of length, 2 cm of width and 2 cm of thickness. The strain was measured using R = 120Ω±0.3% strain gauges (Fortunier 2003 and Bertholet 1974) connected in an half Wheatstone bridge as indicated in Fig. 2. On every specimen was fixed symmetrically two strain gauges. The strain was converted into deformation using the strain bridge EI 616 from DELTALAB. The creep lasted for 10 hours and the recovery for 40 hours. The temperature and relative humidity of the test room are monitored by the electronic thermo-hygrometer, model ETHG913R from Oregon Scientific.

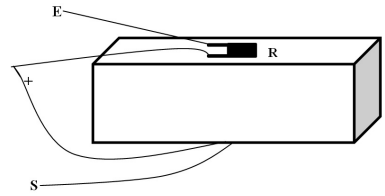

Fig. 2: Rectangular beam carrying two symmetrical gauges.

On this Fig. 2, E and S represent the gauge electrodes that are directly connected to the strain bridge and R stands for the gauge electrical resistance. During the test the sample is lain

on the test machine in such a way that one gauge is on the top and another one symmetrically on the opposite face of the sample.

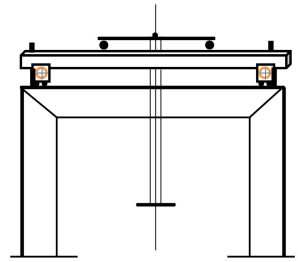

Fig. 3: Bending creep testing device.

The device used for the bending creep test is illustrated by the diagram in Fig. 3. The device setup was inside the air-condition room. Each specimen was placed horizontally on the two supporting points of the device. The distance between the supporting points was 340 mm. A symmetrical load was applied at each of the third-points of the specimen. At the supporting points and at the loading points, we used a cylinder made of steel, to press the surfaces of the beam, in order to minimize the perpendicular shearing strain. We tested all the three samples with eight different loads. But in this paper, we just present the results obtained with a constant load of 35 kg which is equivalent to a constant stress of σ = 12.86 MPa. Because we wanted to test the performance of the predictor-corrector Kalman filter applied to a biomaterial.

RESULTS AND DISCUSSION

We first carried out a 10 hours creep test with three different samples of Sapelli previously mentioned under a constant stress of σ = 12.86 MPa. Our software had been programmed to measure the deformation after one second. So from the previously modelling of the system, it comes that T = 1 s. The deformations were measured with a square of standard deviation of $b_1^2 = 225 \cdot 10^{-8}$ and the square of standard deviation on the speed of deformation was $b_2^2 = 6{,}25 \cdot 10^{-8}$. The known input of our system u is the acceleration of the creep and the value is $u = 10^{-8}$ m/m/s^2.

From Eq. 17 since at the step k + 1 the deformation is proportional to the acceleration of creep, the only value that suits the simulation processes is the coefficient 0.5. We can consider this parameter as the link between the deformation and the creep acceleration. Then, the maximum variance on the deformation is $\tilde{\varepsilon}^2 = 2{,}5.10^4$ and since $\dot{\varepsilon}_{k+1} \square 1.\ddot{\varepsilon}$ (that is the speed is directly proportional to the acceleration) then, the maximum variance on the speed of deformation is $\tilde{\dot{\varepsilon}}^2 = 10^{-5}$. The various matrices used during the creep test in the Kalman filter are:

$$A = \begin{pmatrix} 1 & 1 \\ 0 & 1 \end{pmatrix}, B = \begin{pmatrix} 0{,}5 \\ 1 \end{pmatrix}, H = \begin{pmatrix} 1 & 0 \\ 0 & 1 \end{pmatrix}, Q = 10^{-6}.\begin{pmatrix} 2{,}5.10^{10} & 5 \\ 5 & 10 \end{pmatrix} \text{ and } R = 10^{-8}.\begin{pmatrix} 225 & 3{,}75 \\ 3{,}75 & 6{,}25.10^{-2} \end{pmatrix}$$

And those used during the recovery phase for the samples are the following:

$$A = \begin{pmatrix} 1 & 1 \\ 0 & 1 \end{pmatrix}, B = \begin{pmatrix} 0{,}5 \\ 1 \end{pmatrix}, H = \begin{pmatrix} 1 & 0 \\ 0 & 1 \end{pmatrix}, Q = 10^{-1}.\begin{pmatrix} 2{,}5.10^{10} & 5 \\ 5 & 10 \end{pmatrix} \text{ and}$$

We present only the results from the sample S1 in order to avoid many figures, all the three samples we tested having similar results.

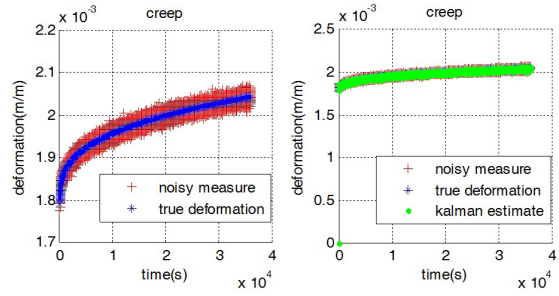

Fig. 4: The left panel shows the true deformation (blue line curve) as well as the measured noisy deformation (red cross curve) for the model. The right panel is similar and show in addition the estimated deformation (green curve) by the Kalman filter.

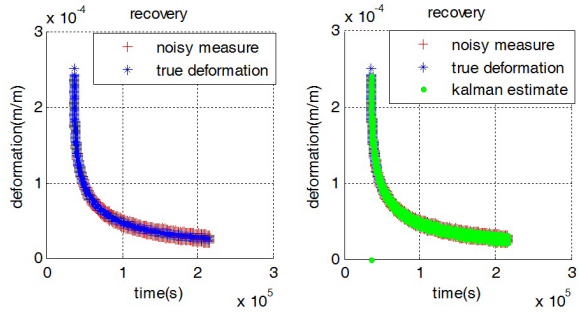

Fig. 5: The left panel depicts the true deformation (blue line curve) as well as the measured noisy deformation (red cross curve) for the model during the recovery. The right panel is similar and shows in addition the estimated deformation (green curve) by the Kalman filter.

From the creep-recovery curves of sample S1 Figs. 4 and 5, we can notice that the estimated deformation and the true deformation are almost too close to distinguish from one another. The noisy-looking curve is the measured deformation. The good agreement between both curves means that the Kalman filter algorithm has removed the noise while retaining the useful deformation. Then the filter converges and has a good response. Several authors studied the creep behaviour of wood species (Talla et al. 2010) and (Pramanick and Sain 2006) but did not take into consideration the influence of noise on the response of their samples. The consequence is that their result may be biased or not enough reliable when compared to our results in this paper.

Figs. 7 and 6 depict the error between the true deformation and the measured deformation, and the error between the true deformation and the Kalman filter's estimated deformation. The measurement error has a standard deviation of about 1.5.10-4 $m.m^{-1}$. It comes out from these figures that the estimated deformation error stays about zero. The consequence is that the Kalman filter has minimized the variance of the estimation error. The behaviour of the discrete Kalman filter applied to creep is similar to its behaviour applied to wild fire (Craig and Mandel 2006) or to electric signals (Simon 2001, Welch and Bishop 2006). This means that the filter is a powerful instrument for creep simulation and lifespan prediction.

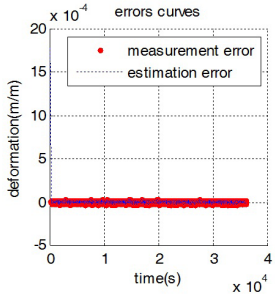

Fig. 6: The estimation error curve of deformation (blue line curve) and the measurement error curve of deformation (red curve) for the model.

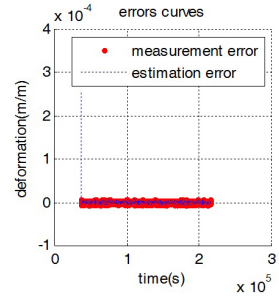

Fig. 7: The estimation error curve of deformation (blue line curve) and the measurement error curve of deformation (red curve) for the model during the recovery phase.

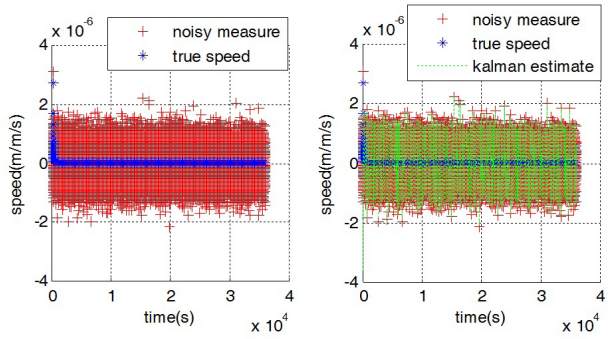

Fig. 8: The left panel shows the true speed of deformation (blue line curve) as well as the measured noisy speed of deformation (red cross curve) for the model. The right panel is similar and depicts in addition the estimated speed of deformation (green curve) by the Kalman filter.

Fig. 8 shows a bonus that we get from the Kalman filter. Since the creep velocity is part of the state $\boldsymbol{x}$, we get a velocity estimate along with the deformation estimate. The creep velocity decreases rapidly at the beginning of the test (that is the primary creep) when the sample is just loaded. During the secondary creep, the velocity remains constant until the end. It was supposed to increase after this creep phase if our test continued until the breaking point. The shape of the speed during the creep test is similar to that obtained by (Dieter 1988) when dealing with mechanical metallurgy and (Doraiswamy 2002). This analogy between our results and the mentioned preceding ones is a proof that Kalman filter is polyvalent.

Figs. 9, 10 depict the characteristics of the gauges noise that perturbs the creep behavior of the samples. It is evident from the histograms curves that both the creep speed and the creep measurement noises are Gaussian.

From the creep-recovery curves of samples S1, S4 and S5 Figs. 4 and 7, we can notice that the estimated deformation and the true deformation are almost too close to distinguish from one another. The noisy-looking curve is the measured deformation. The good agreement between both curves means that the Kalman filter algorithm has removed the noise while retaining the useful deformation. Then the filter converges and has a good response.

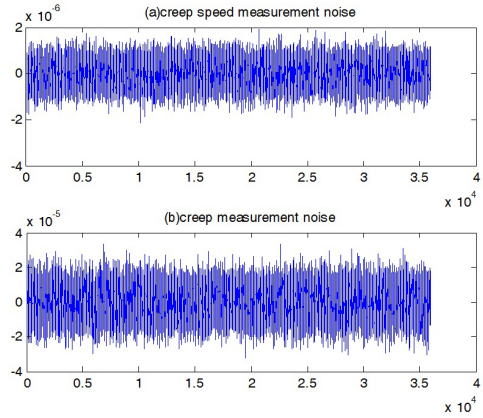

Fig. 9: Panel (a) depicts the measurement noise that perturbs the creep speed and panel (b) shows the measurement noise that perturbs the deformation of the samples.

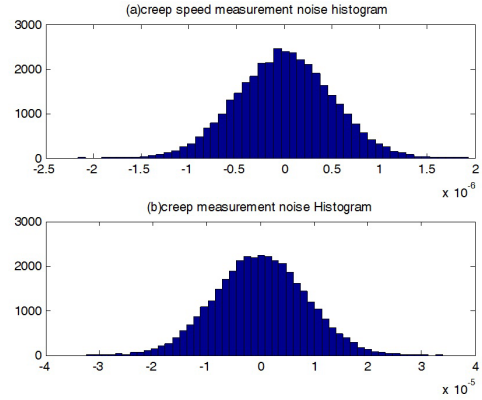

Fig. 10: Panel (a) shows the histogram of the creep speed measurement noise and panel (b) depicts the histogram of the creep or deformation measurement noise.

Figs. 6 and 7 depict the error between the true deformation and the measured deformation, and the error between the true deformation and the Kalman filter's estimated deformation. The measurement error has a standard deviation of about $1.5.10^{-4}$ m/m. It comes out from these figures that the estimated deformation error stays about zero. The consequence is that the Kalman filter has minimized the variance of the estimation error.

Fig. 8 shows a bonus that we get from the Kalman filter. Since the creep velocity is part of the state x, we get a velocity estimate along with the deformation estimate. The creep velocity decreases rapidly at the beginning of the test (that is the primary creep) when the sample is just loaded. During the secondary creep, the velocity remains constant until the end. It was supposed to increase after this creep phase if our test continued until the breaking point.

Figs. 9 and 10 depict the characteristics of the gauges noise that perturbs the creep behavior of the samples. It is evident from the histograms curves that both the creep speed and the creep measurement noises are Gaussian.

CONCLUSIONS

Our task was to implement the discrete Kalman filter under matlab language to estimate the creep behaviour of *Entandrophragma cylindricum*. From the numerical results of simulation, it comes out that the variance of the estimation error is near zero, the estimate and the state have the same expectation value meaning that our estimate is not biased. These results are in perfect agreement with the rules that describe the filter (Kalman 1960, Welch and Bishop 2006). This work demonstrates the workings of the Kalman filter applied to a biomaterial and it is evident that the filter has a good response since the estimate appears considerably smoother than the noisy measurements. So this method of estimation is powerful and efficient than that the Burger's and Schapery's models of creep prediction carried out by (Talla et al. 2010).

REFERENCES

1. Atchounga, P. K., 2013 : Analyse du comportement non linéaire à long terme de *Entandrophragma cylindricum*, Mémoire de master, Université de Dschang Pp 41-60.
2. Basquin, R., 1990 : Mécanique, deuxième partie, Delagrave Pp 247-249, 271.
3. Bertholet, A., 1974 : Jauges d'extensométrie, Laboratoire du génie civil, Place du Levant 1, 1348 Louvain-la-Neuve. Encyclopédie VISHAY d'analyse des contraintes, http://www.vishay.com/strain-gages/.
4. Brown, R. G., Hwang, P. Y. C., 1992: Introduction to random signals and applied Kalman filtering. Second edition, John Wiley & Sons, Inc. Pp 4-5
5. Craig, J. Johns, Mandel, J., 2006: A two stage ensemble Kalman filter for smooth data assimilation, Journal of data science 4: 21-37.
6. Simon, D., 2001: Kalman filtering, Embedded systems programming 14: 72-79.
7. Dieter G. E., 1988: Mechanical metallurgy. Mc Graw-Hill book company, Pp 152-160.
8. Doraiswamy, D., 2002: The origins of Rheology, a short historical excursion. Rheology bulletin 71(1): 1-9.
9. Evensen, G., 2003: The ensemble Kalman filter, Theoretical formulation and practical implementation, Ocean Dynamics 53: 343-367.
10. Fortunier, R., 1998: Mécanique des milieux continus, Cours ENSM-SE. Pp 173-180.
11. Fortunier, R., 2003: Comportement Mécanique des Matériaux.
12. Jacobs, O. L. R., 1993: Introduction to control theory, 2nd edition, Oxford University press Pp 50-60.
13. Jazwinski, A. H., 1970: Stochastic processes and filtering theory, Academic Press, New York Pp 97-102.
14. Fanchon, J. L., 2001 : Guide de mécanique, Nathan, (ISBN 2-09-178965-8), Pp 427- 432.
15. Kalman, R. E., 1960: A new Approach to linear filtering and prediction problems, Journal of basic engineering 82 (Series D), 8: 35-45.
16. Lemaitre, J., Chaboche, J. L., 1988: Mécanique des matériaux solides 2nd, Dunod-Bordas.
17. Maybeck, P., S., 1970: Least squares estimation: from Gauss to Kalman. IEEE spectrum 7: 63-68.
18. Montheillet, F., Moussy, F., 1986: Physique et mécanique de l'endommagement, Éditions de physique, travaux du GRECO grandes déformations 253pp.
19. Mvogo, J. K., 2008 : Regroupement mécanique par méthode vibratoire des bois du bassin du Congo, Thèse de doctorat PhD, 25pp

20. Pramanick, A., Sain, M., 2006: Temperature-stress equivalency in nonlinear vicoelastic creep characterization of thermoplastic/Agro-fiber composites, Journal of Thermoplastic Composites Materials 19:12-13.
21. Talla, P.K., Foadieng, E., Fogue,M., Mabekou, J.S., Pelap, F.B.,. Sinju, A.F., Foudjet. A, 2010: Nonlinear creep behavior of *Raphia vinifera* L. *Arecacea* under flexural load, International Journal of Mechanics and Solids 5(2): 151-172.
22. Welch, G., Bishop, 2006: An introduction to the Kalman filter. TR 95-041, Department of computer science, University of North Carolina at Chapel Hill, Chapel Hill, NC 27599-3175, Pp 3-6.
23. Zhao, Y., Bo Liang, B., Iwnicki, S., 2014: Friction coefficient estimation using an unscented Kalman filter, International Journal of Vehicle Mechanics and Mobility 52(1): 53-70.

Pierre Kisitotalla*, Prisca Kuida Atchounga, Blaise Mtopi
University of Dschang
Department of Physics
Laboratory of Mechanics and Modelling of Physical Systems (*L2MSP*)
P.O. Box 69 Dschang
Cameroon
Corresponding author:tpierrekisito@yahoo.com
Phone: (+237) 674 78 4870